Asociación Argentina
de Mecánica Computacional

Mecánica Computacional Vol XXXIX, págs. 727-736 (artículo completo)
F.E. Dotti, M. Febbo, S.P. Machado, M. Saravia, M.A. Storti (Eds.)
Bahía Blanca, 1-4 Noviembre 2022

EFFECT OF STRESS TRIAXIALITY ON THE COMPUTATION OF THE COLLAPSE PRESSURE OF SUBMARINE PIPES

Felipe T. Stumpf[a], Matheus F. Kuhn[b], Allan R. de P. Dias[b], Thomas G. R. Clarke[b], Håvar Ilstad[c], Erik Levold[c] and Ignacio Iturrioz[a]

[a]*Department of Mechanical Engineering, Federal University of Rio Grande do Sul. Rua Sarmento Leite, 425, Porto Alegre, Brazil*

[b]*Physical Metallurgy Laboratory(LAMEF), Federal University of Rio Grande do Sul. Av. Bento Goncalves, 9500, prédio 43820, Porto Alegre, Brazil*

[c]*Equinor ASA, Arkitekt Ebbells veg 10, Trondheim, 7053 Ranheim, Norway*

Keywords: metallic pipelines, stress triaxiality, offshore structures, thick-walled pipes.

Abstract. The linepipe steel engineered for ultra-deepwater fluid transportation undergo extreme conditions due the high pressure. One major concern of pipeline engineers when designing pipelines for such environment is to predict the onset of buckling caused by the static external hydrostatic pressure. DNV-ST-F101 standard features as one of the most popular guides for the pipelines project and presents the design equation for the prediction of the collapse capacity of submarine pipelines covering a limited diameter-to-thickness (D/t) range leaving heavy-walled pipes, such as those demanded for the presalt exploration, out of the scope. The accuracy of the DNV-ST-F101 design equation is investigated in the scope of this research paper for pipes featuring D/t lower than 15, defined as the lower bound covered by the standard, and it is found that it underestimates the maximum collapse capacity in those cases possibly driving the pipe operators to define pipe walls excessively thick causing the cost increasing of the operation. We sustain that the major cause for such inadequacy falls into the standard's equation for the pipe's plastic collapse, which uses the material's yield strength to set the beginning of the plastic collapse. Using the finite element method we conclude that the high level of stress triaxiality inside the pipe's wall at the moment of collapse calls for the necessity of a different parameter to measure the onset of plastic failure. Numerical data of five different metallic materials and five different pipe configurations are used to propose an alternative equation to compute the plastic collapse of pipes subjected to external pressure, and our results consistently improve the accuracy of DNV's approach for moderate to thick pipes without compromising the results of thinner structures.

1 INTRODUCTION

The new frontiers for the offshore oil exploration have presented new challenges to the production and transportation industry to cope with the extreme conditions found in the ultra-deepwater conditions, such as those found in High Temperature/High-Pressure wells (HT/HP) found in Brazilian territorial waters, and pointed as the harshest environments for the exploration due to the synergy of temperature, pressure, high concentrations of H_2S and CO_2 that are knowingly for damaging the pipeline materials (Shadravan and Amani , 2012; Denney , 2013). Within this context, research institutes have struggled along with mill companies to produce line pipe steel alloys with greater wall thicknesses to fulfill the requirements of strength for service under those environmental conditions.

Among several different failure modes that a submarine pipeline can experience, its structural collapse can be thought as one of the most damaging, both for the operating company and for the environment. A complete review on different failure events experienced by the industry concerning pipelines, risers, and umbilical cables can be found in Drumond et al. (2018).

DNV-ST-F101 (DNV , 2021) treats elastic (dominant in thinner pipes) and plastic (dominant in thicker pipes) effects separately and utilizes the formulation proposed by Haagsma and Schaap (1981) to combine those effects into a collapse pressure for steel pipes. Although DNV's approach has been widely (and successfully) used in the design of steel pipelines for offshore applications for the past decades, it is understood that its formulation is originated from simple fundamental mathematics with expressions generated to blend transitions between elastic and plastic collapse. The expressions were shown to accurately predict the collapse pressure of the great majority of installed pipelines, however, in the present context of offshore applications in increasingly deeper waters, this formulation is being put to proof for the upcoming necessity of thicker configurations.

We propose an alternative, analytical approach for the computation of the so-called plastic collapse pressure, which dominates the failure mode for thicker pipes. Although simple, our proposal shows to be capable of improving the prediction of the structural collapse of moderate to thick metallic pipes under external hydrostatic pressure without compromising DNV's well known accuracy for thinner structures.

The beginning of the investigations around submarine pipes and different aspects such as their design, fabrication, installation and operation dates back to the 1970s. One can cite the pioneer work carried out by Palmer and Martin (1975), in which they address the issue of buckling pipes under bending and external hydrostatic pressure. This combination of structural loads, if taken to a certain limiting magnitude, can lead to a sudden change of the original pipe's circular-shaped cross section into an ovalised one, which is called *buckling*. It is an instability phenomenon. When no (or negligible) bending acts on the structure, the external pressure that leads to buckling is called *collapse pressure*, defined here as P_{co}.

The prediction of collapse of moderate to thick pipes ($D/t < 20$) gained considerable attention over the past decades (DNV , 2014). The finite element method was used to study the combined effects of hydrostatic pressure, bending and tension on the collapse of thick pipelines by Bai et al. (1997). Estefen (1999) performed experimental and numerical analyses considering both damaged and undamaged pipes taking into account the effect of reel-lay procedure of installation. Li et al. (2019) presented an analytical approach for the problem by solving directly the stability equations of a plane strain case of deformation and Li et al. (2021) solved the same problem for a full 3D problem. Based on the thick shell theory, Yu et al. (2019) presented an approach to determine the collapse pressure of thick pipes.

The general collapse of pipes by hydrostatic pressure (no bending or axial loads) is defined as being composed by two components: the elastic collapse and the plastic collapse, and their contributions is governed by the D/t ratio. Plastic effects are dominant in thick pipes and a plastic collapse pressure P_{pl} is computed as

$$P_{pl} = \alpha_{fab}\, 2\sigma_y \frac{t}{D} \tag{1}$$

where α_{fab} is a parameter that takes into account the fabrication process of the pipe and varies from 0.85 to 1.00 for UOE and seamless manufacturing processes (in the study here presented we consider $\alpha_{fab} = 1$), D and t are the pipe's external diameter and thickness, respectively, and σ_y is the material's yield stress.

Elastic phenomena, on the other hand, governs the collapse in thin pipes, and the expression of the elastic collapse pressure P_{el} is

$$P_{el} = 2\frac{E}{1-\nu^2}\left(\frac{t}{D}\right)^3 \tag{2}$$

in which ν is the Poisson's ratio and E the Young's modulus of the material.

The structural failure of the pipeline takes place at the collapse pressure P_{co}, which is understood to combine both plastic and elastic phenomena. The equation for P_{co} was originally proposed by Haagsma and Schaap (1981) and later adopted by DNV (2021) and reads

$$\left(P_{co} - P_{el}\right)\left(P_{co}^2 - P_{pl}^2\right) = P_{co}P_{el}P_{pl}f_o\frac{D}{t} \tag{3}$$

in which f_o is the ovalisation factor of the pipe to take into account geometrical imperfections caused during fabrication or installation, and is computed as

$$f_o = \frac{D_{max} - D_{min}}{D_{nom}}\,, \tag{4}$$

being D_{min}, D_{max} the minimum and maximum measured diameters of the pipe, respectively, and D_{nom} its nominal diameter.

2 NUMERICAL VERSUS ANALYTICAL COLLAPSE PRESSURE

In order to evaluate the accuracy of the analytical solution of equation (3), we undertake a set of 3D finite element simulations using the commercial package Simulia Abaqus (Abaqus/CAE , 2014). To that end, we choose five different high strength steel alloys commonly used in pipeline construction: API X52, X60, X65, X70 and X80. In all simulations the pipes have a 323.85mm (12.75") diameter, 4% ovalisation and 0% eccentricity. Additionally, five different D/t ratios are covered: $D/t = [7.5, 10, 15, 20, 30]$. The materials are described by the tension stress-strain curves fitted to the Ramberg-Osgood model (Ramberg and Osgood , 1943)

$$\epsilon(\sigma) = \frac{\sigma}{E}\left[1 + \alpha\left(\frac{\sigma}{\sigma_y}\right)^{n-1}\right] \tag{5}$$

with the parameters listed in Table 1 with each source in the literature.

The boundary conditions are illustrated in Figure 1 along with the mesh used in the simulation, which we defined after a mesh convergence study (here omitted to keep the paper

Alloy	E [GPa]	σ_y [MPa]	σ_u [MPa]	n	α	Source
X52	208	375	468	15.6	1.21	Shuai et al (2018)
X60	206	415	520	10.9	1.4	Trifonov (2015)
X65	207	450	604	13.7	1.31	Bastola et al. (2014)
X70	210	537	620	15.1	0.96	Bastola et al. (2014)
X80	217	544	631	13	1.33	Lower (2014)

Table 1: Parameters used as input in equation (5) to model stress-strain behavior of each material.

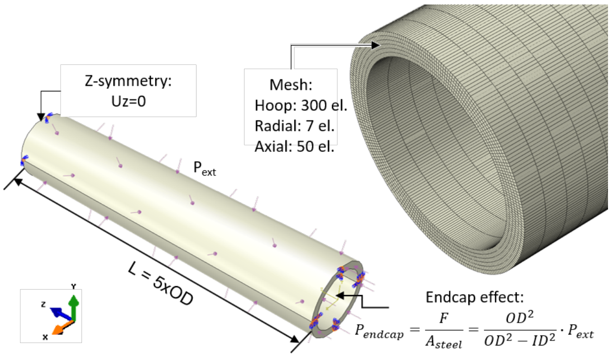

Figure 1: Boundary conditions and finite element mesh applied to all the simulations.

concise). The simulated pipes are discretized by first order reduced integration solid elements named C3D8R in Abaqus (Abaqus/CAE , 2014). Figure 1 also shows the external pressure applied to the structure in the form of purple arrows surrounding the pipe with the definition assumed to compute the endcap effect at the pipe ends.

Figure 2 shows the comparison between analytical and numerical results of the collapse pressure P_{co} for all steel grades analyzed. It can be seen that for greater D/t ratios the agreement between numerical and analytical results are acceptable, but for moderate to thick pipes ($D/t < 17.5$) the use of equations (1)-(3) tends to underestimate P_{co}, leading to overly conservative results, which in turn may lead to relatively conservative wall-thickness design of offshore pipelines. This finding is also reported in Stark and McKeehan (1995); Liessem et al. (2007); Toscano et al. (2003); DeGeer et al. (2004); Wolodko and DeGeer (2006); Palmer and King (2008); Benjamin and Cunha (2012); Shun-Feng et al. (2012); Bastola et al. (2014).

3 WHY DON'T ANALYTICAL AND NUMERICAL RESULTS AGREE FOR MODERATE TO THICK PIPES?

It is important to point out that DNV's equation for the collapse pressure (equation (3)) takes into account the simultaneous contribution of the elastic and plastic collapse mechanisms, controlled by equations (2) and (1), respectively. We emphasize that the origin of equation (1) is the famous expression for the hoop stress σ_h acting on the wall of cylindrical shells considering membrane behavior, which reads

$$\sigma_h = \frac{PD}{2t} \tag{6}$$

in which P is the external (or internal) pressure acting on the cylinder. Equation (1) is merely equation (6) rearranged and written in terms of the yield stress σ_y instead of of the pressure. Therefore, the physical interpretation of equation (1) is that *the plastic collapse takes place when the stress in the hoop direction inside the pipe's wall (subjected to external pressure)*

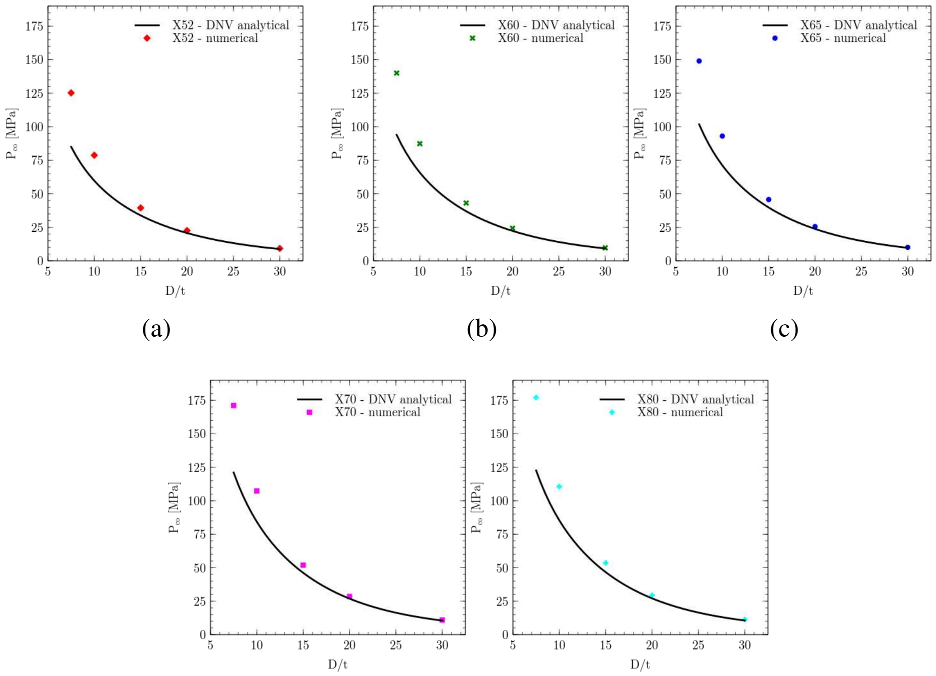

(a) (b) (c)

(d) (e)

Figure 2: Comparison between analytical results using equation (3) and numerical simulations using 3D FEM models for (a) X52, (b) X60, (c) X65, (d) X70 and (e) X80 grade steels.

reaches the material's yield strength, which is known to be a scalar parameter usually determine during tensile *uniaxial* tests. Furthermore, it is well known that the accurate use of equation (6) is restricted to thin-walled vessels.

With that in mind, we propose the following question: *is σ_y the best suited parameter to measure the plastic collapse of pipes subjected to external pressure loads?* In the following section we come up with arguments to sustain a negative answer to that question and propose a modification to the computation of P_{pl}.

- **Stress triaxiality**

Unlike samples under uniaxial tensile tests (which experiment a *uniaxial* stress state), the stress state inside highly confined structures can reach a very high level of *triaxiality*. The walls of pipes under high external hydrostatic pressure loads fall into the second category due to its state of considerable confinement. This effect (stress triaxiality) is much more severe for thick pipes than for thin pipes.

A good measure of the triaxiality level is the stress triaxiality factor (TF) defined as the ratio of hydrostatic stress σ_{hyd} to the equivalent von Mises stress σ_{vM}, which, in terms of the principal stresses σ_1, σ_2 and σ_3 reads as

$$TF = \frac{\sigma_{hyd}}{\sigma_{vM}} = \frac{\sqrt{2}}{3}\frac{\sqrt{\sigma_1+\sigma_2+\sigma_3}}{\sqrt{(\sigma_1-\sigma_2)^2+(\sigma_1-\sigma_3)^2+(\sigma_2-\sigma_3)^2}}. \tag{7}$$

Sajid and Kiran (2018) make use of TF to conclude that *"the ultimate tensile strength of structural steels...increase linearly with increase in stress triaxiality"* and that *"an increase up to 54% in ultimate tensile strength is observed for all the three structural steels considered in* (their) *study when the (TF) is increased from* 0.34 *to* 0.88*"*.

	X52: ($\sigma_y = 375$ MPa , $\sigma_u = 468$ MPa)					X60: ($\sigma_y = 415$ MPa , $\sigma_u = 520$ MPa)				
D/t	σ_r [MPa]	σ_h [MPa]	σ_a [MPa]	σ_{vM} [MPa]	TF	σ_r [MPa]	σ_h [MPa]	σ_a [MPa]	σ_{vM} [MPa]	TF
7.5	-122	-629	-381	439	**0.86**	-136	-728	-441	512	**0.85**
10	-75	-553	-319	414	**0.76**	-83	-626	-360	470	**0.76**
15	-37	-500	-270	401	**0.67**	-41	-561	-301	451	**0.67**
20	-21	-481	-255	398	**0.63**	-23	-537	-282	445	**0.63**
30	-9	-461	-234	391	**0.60**	-9	-511	-256	435	**0.59**

	X65: ($\sigma_y = 450$ MPa , $\sigma_u = 604$ MPa)					X70: ($\sigma_y = 537$ MPa , $\sigma_u = 620$ MPa)				
D/t	σ_r [MPa]	σ_h [MPa]	σ_a [MPa]	σ_{vM} [MPa]	TF	σ_r [MPa]	σ_h [MPa]	σ_a [MPa]	σ_{vM} [MPa]	TF
7.5	-139	-714	-425	498	**0.86**	-164	-854	-515	598	**0.85**
10	-89	-661	-378	495	**0.76**	-101	-765	-434	575	**0.75**
15	-42	-590	-308	475	**0.66**	-48	-695	-362	561	**0.66**
20	-23	-558	-265	464	**0.61**	-27	-669	-337	556	**0.62**
30	-9	-546	-262	465	**0.59**	-11	-649	-323	553	**0.59**

	X80: ($\sigma_y = 544$ MPa , $\sigma_u = 631$ MPa)				
D/t	σ_r [MPa]	σ_h [MPa]	σ_a [MPa]	σ_{vM} [MPa]	TF
7.5	-163	-855	-515	599	**0.85**
10	-105	-790	-448	593	**0.75**
15	-50	-720	-381	580	**0.66**
20	-27	-689	-350	573	**0.62**
30	-16	-644	-295	545	**0.58**

Table 2: Different stress components and the triaxiality factor at the most external layer of pipes at the moment of collapse.

We investigate the stress levels at a pipes' walls at the moment when the collapse takes place. Axial, radial and hoop components of stress (σ_a, σ_r and σ_h, respectively) at the most external layer of the pipe are monitored in order to compute the triaxiality factor TF for each different combination of material and D/t ratios. Shear stresses are negligible and, therefore, could be neglected in the present work.

The results for TF highlighted in boldface in Table 2 indicate a high level of triaxiality (approximately 0.85) for the thicker configuration ($D/t = 7.5$), which according to the exposed in the beginning of this section, means that the materials collapse with stresses much higher than σ_y.

In Figure 3(a) we plot the stress state at the most external layer in the pipes' walls of each pipe (for $D/t = 7.5$) at the moment of collapse together with the stress state during the uniaxial experiments used to determine the yield strength σ_y of X52, X60, X65, X70 and X80 grade steels. We choose to do so in the p-q domain, i.e., ploting hydrostatic ($p = \sigma_{hyd}$) versus the deviatoric ($q = \sigma_{vM}$) stresses. This is interesting because it makes it easier for one to visualize the difference in TF (which, in this case, is proportional to the slope of the curves) for *uniaxial versus triaxial* cases of stress distribution. Note that at the moment of collapse all pipes experiment a higher deviatoric (von Mises) stress compared to the materials' yield stress, in a ratio not higher than 20% (see Table 2).

The diagram in Figure 3(b) brings a graphical representation of the results for TF presented in Table 2. In Figure 3(c) we display the ratio σ_h/σ_y at the moment of collapse in terms of the triaxiality factor. It becomes obvious that thicker pipes (greater TF) collapse with hoop stresses up to at least 50% larger than σ_y, independent on the pipes' material.

Bearing in mind that equation (1) for the plastic collapse pressure P_{pl} uses σ_y as a measure for the occurrence of the structural failure (expression, it is worth recalling, that has its origin in the hoop stress acting on the walls of thin cylindrical shells), we come to the answer of the previously proposed question: *is σ_y the best suited parameter to measure the plastic collapse of pipes subjected to external pressure loads?* ***No, it is not. And the reason is the level of stress triaxiality acting on the pipes' walls.***

These observations will be helpful in section 4 where we propose a modification to equation

(1), which must take into account the wall's thickness and is independent on the pipe's material.

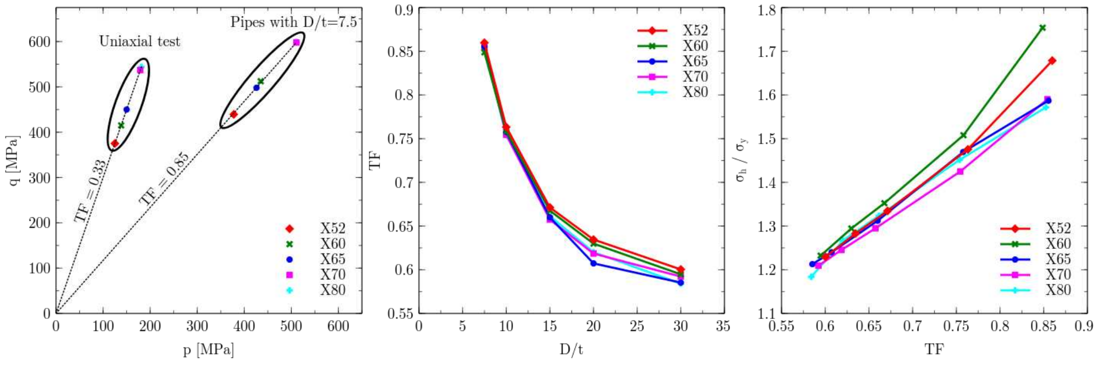

(a) (b) (c)

Figure 3: (a) Stress state (in p-q domain) in the samples during uniaxial test and at the external layer of the pipes' walls (for $D/t = 7.5$) at the moment of collapse.(b) triaxiality factor versus D/t at the moment of collapse. (c) increase in the ratio σ_h/σ_y with the increase in TF at the moment of collapse.

4 MODIFICATION TO THE EQUATION FOR P_{PL}

Our proposal is to present an alternative candidate to σ_y to control the onset of the plastic failure, whose effect on P_{pl} can be weighted according to the pipes' D/t ratio.

In Figure 4 we put together the results of Figures 3(b) and 3(c) and plot the ratio σ_h/σ_y in terms of D/t. The generated data allows for the interpolation of a power law curve, as plotted in the dotted line of Figure 4, according to

$$\sigma_h = 2.5\,\sigma_y \left(\frac{D}{t}\right)^{-0.22} . \tag{8}$$

We use this result to construct the *modified* plastic collapse pressure P_{pl}^{modif}

$$P_{pl}^{modif} = \alpha_{fab}\,2\,\sigma_h \frac{t}{D} = 5\,\alpha_{fab}\,\sigma_y \left(\frac{t}{D}\right)^{1.22} , \tag{9}$$

and compute the *modified* collapse pressure P_{co}^{modif}

$$\left(P_{co}^{modif} - P_{el}\right)\left(\left(P_{co}^{modif}\right)^2 - \left(P_{pl}^{modif}\right)^2\right) = P_{co}^{modif} P_{el} P_{pl}^{modif} f_0 \frac{D}{t} \tag{10}$$

The new set of equations (8)-(10) is used to compute the (new) proposed analytical solutions of the collapse pressure of the same pipes' configurations that we have detailed in Section 2, whose original results (using equations (1)-(3)) are shown in Figure 2. The boundary conditions, meshes and material parameters are kept the same. Figure 5 shows the obtained results, in which the solid lines regarding DNV-analytical solution were kept for the sake of comparison. The dotted lines refer to the proposed modification of equations (8)-(10).

It can be seen that the proposed equations (8)-(10) successfully account for the stress triaxiality, increasing the collapse pressure for configurations with lower D/t ratios. On the other

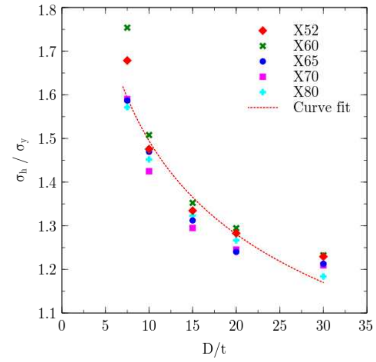

Figure 4: Power law curve interpolating the data at the moment of collapse.

hand, P_{co} of pipes with moderate to high D/t ratios in which stress triaxiality does not play an important role, are less impacted by the present proposal. In Table **??** we summarize the relative error when equations (3) and (10) are used in comparison to the numerical results.

As it can be seen, the error reduction is more effective for smaller values of D/t, reaching a reduction of more than three times in some cases. For example, for X65 the error using DNV's equation (3) was 31.7%, while when using our proposal the error was reduced to 7.7% for $D/t = 7.5$. In the case of higher D/t ratios, the classical equation (3) already leads to good results, so the improvement in using equation (10) is less significant.

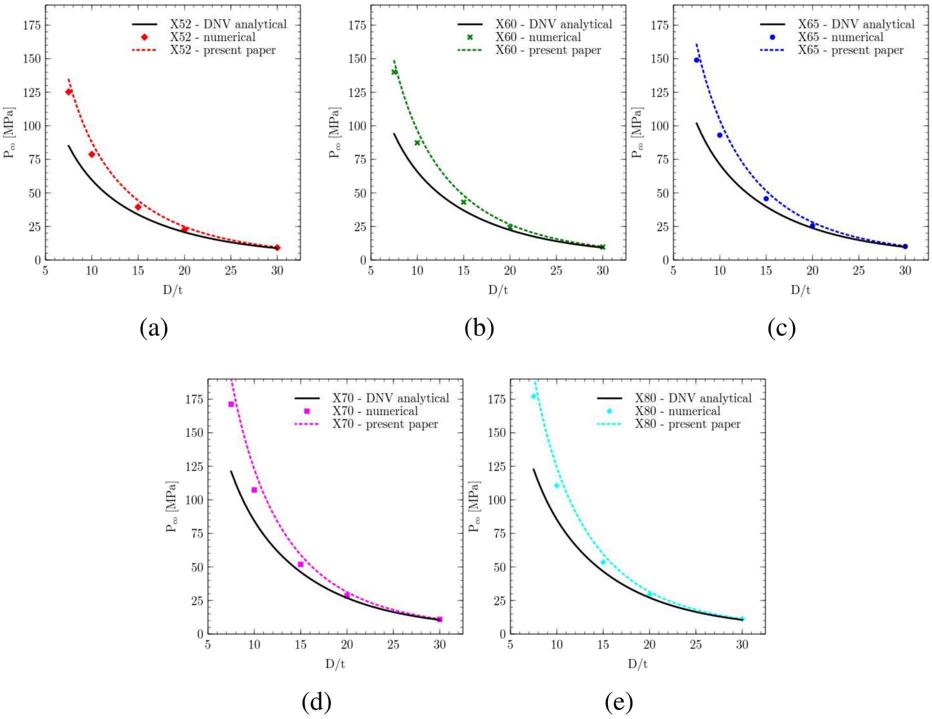

(a) (b) (c)

(d) (e)

Figure 5: Analytical results for the collapse pressure using equation (10) in dotted lines, analytical (DNV) results using equation (3) in solid lines, and numerical simulations using 3D FEM models for (a) X52, (b) X60, (c) X65, (d) X70 and (e) X80 grade steels.

5 CONCLUSIONS

DNV's equations were shown to underestimate the collapse pressure of pipes subjected to external pressure, leading to overly conservative results, especially for greater wall thicknesses. Our results show that the use of the yield strength as a measure for the onset of the plastic collapse of these structures is not the best suited approach, since it is obtained during *uniaxial* tests, and the wall of an actual pipe can undertake a highly *triaxial* stress state. This triaxiality is responsible for postponing the occurrence of the pipe's plastic collapse.

For that reason, we propose a modification to DNV's analytical equations for the plastic collapse pressure and the collapse pressure, taking into account the stress triaxiality inside the pipe's wall. Making use of an auxiliary power law expression, it is shown possible to analytically determine the collapse pressure more accurately. This expression relates the D/t ratio of the pipe with the ratio between its hoop stress and its yield stress at the moment of collapse. It does not introduce any significant extra complexity and the equation is, as the original one, material independent.

ACKNOWLEDGMENTS

This work was supported by Equinor in association with the University of Rio Grande do Sul, LAMEF – Physical Metallurgy Laboratory, and GMAp – Applied Mechanics Group. In addition, the authors wish to thank the National Council for Scientific and Technological Development (CNPq – Brazil) and Coordination for the Improvement of Higher Education Personnel (CAPES – Brazil), FAURGS (Fundação de Apoio da Universidade Federal do Rio Grande do Sul), and the Brazilian National Agency of Petroleum, Natural Gas and Biofuels (ANP) for their support.

REFERENCES

Abaqus/CAE, Manual software version 6.14-1, *Dassault Systèmes Simulia Corp.* 2014.

Bai Y, Igland RT and Moan T. Tube collapse under combined external pressure, tension and bending. *Marine Structures* 1997; 10:389-410.

Bastola A, Mirzaee-sisan A, Wang J and Njuguna J. Predicting Hydrostatic Collapse of Pipes Using Finite Element Analysis. *Proceedings of the ASME 2014 33th International Conference on Ocean, Offshore and Arctic Engineering. Volume 6A: Pipeline and Riser Technology.* San Francisco, USA. June 8–13, 2014. V06AT04A048.

Benjamin AC and Cunha DJ. Assessment of Hydrostatic Collapse of Submarine Pipelines: The Classical Approach Revisted. *Proceedings of the 31st International Conference Offshore Mechanics and Arctic Engineering.* Rio de Janeiro, Brazil. July 1-6, 2012. OMAE2012-83833.

DeGeer D, Marewski U, Hillenbrand H-G, Weber B and Crawford M. Collapse testing of thermally treated line pipe for ultra-deepwater applications. *Proceedings of the 23rd International Conference Offshore Mechanics and Arctic Engineering.* British Columbia, Canada. June 20–25, 2004. OMAE2004-51569.

Denney D. Offshore HP/HT Gas Well: Drilling and Well Testing. *Journal of Petroleum Technology* 2013; 65:111-115.

Det Norske Veritas. *Joint Industry Project Proposal: Collapse Assessment of Offshore Pipelines With* $D/t < 20$. 2014.

Det Norske Veritas. *DNV-ST-F101 - Submarine pipeline systems*. 2021.

Drumond GP, Pasqualino IP, Pinheiro BC and Estefen SF. Pipelines, risers and umbilicals failures: A literature review. *Ocean Engineering* 2018; 148:412-425.

Estefen SF. ollapse behaviour of intact and damaged deepwater pipelines and the influence of the reeling method of installation. *Journal of Constructional Steel Research* 1999; 50:99-114.

Haagsma SC and Schaap D. Collapse Resistance of Submarine Pipelines Studied. *Oil and Gas Journal* 1981; 79:86-95.

Li Z, An C and Duan M. An analytical approach for elastic and non-elastic buckling of pipes under external/internal pressures. *Ocean Engineering* 2019; 187:106160.

Li Z, Duan M and An C. An improved analytical solution for elastic and elastic-plastic buckling of pipes under hydrostatic pressures. *Ocean Engineering* 2021; 230:109009.

Liessem A, Grob-Weege J, Knauf G and Zimmermann S. UOE Pipes for Ultra Deep Water Application — Analytical and FE Collapse Strength Prediction vs. Full-Scale Tests of Thermally Treated Line Pipe. *Proceedings of the 7th International Society of Offshore and Polar Engineers* Lisbon, Portugal.

Lower M. *Strain-Based Design Methodology of Large Diameter Grade X80 Linepipe*. Report ORNL/TM-2014/106, US Department of Energy, 2014.

Palmer AC and King RA. *Subsea Pipeline Engineering*. Pennwell Books, Tulsa, 2008.

Palmer AC and Martin JH. Buckle Propagation in Submarine Pipelines. *Nature* 1975; 254:46-48.

Ramberg W and Osgood WR. Description of Stress-Strain Curves by Three Parameters. *NASA* 1943.

Sajid HU and Kiran R. Influence of high stress triaxiality on mechanical strength of ASTM A36, ASTM A572 and ASTM A992 steels. *Construction and Building Materials* 2018; 176:129-134.

Shadravan A and Amani M. HPHT 101-What Petroleum Engineers and Geoscientists Should Know About High Pressure High Temperature Wells Environment. *Energy Science and Technology* 2012; 4:36-60.

Shuai Y, Shuai J and Zhang X. Experimental and numerical investigation of the strain response of a dented API 5L X52 pipeline subjected to continuously increasing internal pressure. *Journal of Natural Gas Science and Engineering* 2018; 56:81-92.

Shun-Feng G, Yuan C, Wei-liang J, Yong B, Zhi-gang L and Gong-yan Z. Local buckling of deepwater oil-gas pipeline under high hydrostatic pressure. *Journal of ZheJiang University (Engineering Science)* 2012; 46(1):14-19.

Stark P and McKeehan D. Hydrostatic Collapse Research in Support of the Oman India Gas Pipeline. *Proceedings of the Offshore Technology Conference*. Houston, USA. 1995. OTC7705.

Toscano RG, Dvorkin EN, Timms CM and DeGeer D. Determination of the collapse and propagation pressure of ultra-deepwater pipelines. *Proceedings of the 22nd International Conference Offshore Mechanics and Arctic Engineering.* Cancun, Mexico. June 8–13, 2003. OMAE2003-37339.

Trifonov OV. Numerical Stress-Strain Analysis of Buried Steel Pipelines Crossing Active Strike-Slip Faults with an Emphasis on Fault Modeling Aspects. *Journal of Pipeline Systems Engineering and Practice* 2015; 6:04014008.

Wolodko J and DeGeer D. Critical buckling conditions for deepwater pipelines. *Proceedings of the 25th International Conference Offshore Mechanics and Arctic Engineering.* Hamburg, Germany. June 4–9, 2006. OMAE2006-92173.

Yu J-x, Han M-x, Duan J-h, Yu Y and Sun Z-z. A modified numerical calculation method of collapse pressure for thick-walled offshore pipelines. *Applied Ocean Research* 2019; 91:101884.